Mikrochim. Acta 131, 35–46 (1999)

Mikrochimica Acta

Fast Response Oxygen Micro-Optodes Based on Novel Soluble Ormosil Glasses

Ingo Klimant*, **Falk Ruckruh, Gregor Liebsch, Achim Stangelmayer,** and **Otto S. Wolfbeis**

University of Regensburg, Institute of Analytical Chemistry, Chemo- and Biosensors, D-93040 Regensburg, Germany

Abstract. A new type of phenyl substituted ormosils as a matrix for oxygen-sensitive micro-optodes is described. The new ormosils combine features of classical polymers such as solubility in organic solvents and those of sol–gel glasses such as mechanical stability and a porous structure. They make possible a simple and fast fabrication of microsensors with reproducible properties. The influence of the conditions during the polymerisation process (precursor composition and thermal treatment) on the sensing properties has been studied in detail. Oxygen-sensitive films with ruthenium(II)–tris-(4,7-diphenyl-1,10-phenanthroline) and platinum(II)–octaethylporphyrin as indicators were characterised with respect to their mechanical and photophysical properties. Photostability, oxygen sensitivity, response behaviour and signal intensities of the sensing films and the micro-optodes were examined. Micro-optodes based on the new sensing materials are fast responding, photostable and can be produced with a sufficient batch to batch reproducibility. Compared to previously described oxygen micro-optodes, where polystyrene was used as immobilisation matrix, the new sensors can be autoclaved and show favourable properties such as a faster response and a higher sensitivity. They possess many potential applications in medical and biological research.

Key words: micro-optode; ormosil; luminescence decay time; oxygen sensing.

The measurement of chemical and physical parameters with high spatial resolution and negligible disturbance of the sample is a typical problem in medical and biological research [1]. Microsensors are powerful tool to solve this problem. Typically such microsensors have tip diameters as thin as 5–10 μm, which provide an almost non-perturbing measurement in intact biological systems.

Microelectrodes for various analytes such as pH, nitrate,nitrous oxide and sulfite were developed over the last twenty years and have been successfully applied to various aquatic systems, tissue and even single cells [2–5].

Dissolved oxygen is a key parameter in biological systems and is either produced by autotrophic photosynthesis in presence of light, or consumed by different metabolism processes. Knowledge of oxygen gradients in complex samples is of paramount importance for understanding and quantification of these processes. Therefore most microsensors described in the literature are oxygen sensors. Needle-type and Clark-type microelectrodes with dimensions of up to a few μm have been described [6, 7]. The Clark-type electrodes in particular display outstanding features such as very small sensitivity to stirring and a very fast response. Their expensive and tedious fabrication and fragility, however, limit a more frequent application of oxygen microelectrodes. Recently fiber optical microsensors (so called micro-optodes) have been presented as an inexpensive alternative to microelectrodes [8, 9]. They are much easier to manufacture, have a better mechanical stability and, depending on the composition of the sensing layer, can give selective measurement of even trace levels of oxygen. The oxygen-sensitive coatings were based on luminescent ruthenium(II)-complexes

* To whom correspondence should be addressed

or phosphorescent platinum(II) porphyrins dissolved in a polystyrene matrix [10–12]. Micro-optodes with ruthenium(II)-tris(4,7-diphenyl-1,10-phenanthroline) ($Ru[dpp]_3$) as indicator are highly luminescent and photostable but suffer from only moderate oxygen sensitivity and long response times compared to microelectrodes ($t_{90} \cong 3s$). On the other hand, sensors based on platinum(II) porphyrin complexes dissolved in polystyrene show an excellent oxygen sensitivity but suffer from only moderate signal intensities, a lower photostability and again a slow response [9].

Here we report on a new type of sol–gel glasses used as matrix for design of fast responding oxygen micro-optodes which combine high signal intensity with sufficient photostability and high quenching efficiency.

Sol–gel derived glasses are attractive matrices for immobilisation of indicators and have already been described for optical sensing of pH, ammonia, ionic species, certain biomolecules and of course oxygen [13]. The sol–gel process allows the non-leachable entrapment of water-soluble indicators without previous chemical modification with lipophilic or reactive groups. It is possible to tailor relevant matrix properties such as pore size distribution, refractive index and analyte permeability by proper adjustment of the pH, temperature and duration of the gelation process [14]. Another outstanding feature of sol–gels is their excellent adhesion to glass and other silica substrates, due to a covalent linkage that is formed with silanol groups of the glass surface.

However, the reproducible fabrication of stable sensor matrices with sol–gel as matrix is not as simple as often described. All parameters have to be kept constant during the manufacturing process. Here the ''advantage'' of a matrix that may be tailored by slight variation of the parameters during the polymerisation turns out to be a disadvantage with respect to obtaining materials with identical sensing properties. Furthermore sensors based on sol–gel entrapped indicators are frequently not stable over time. Drifts of the calibration curves have been observed, caused by aging of the sol–gel matrix. This may be explained as due to continuous condensation of free silanol groups over time and a consequent densification of the matrix.

Although frequently described, sol–gels based on pure tetraethoxysilane as precursor are not at all the optimal matrix for oxygen optodes [15, 16]. The sensitivity of such sensors in aqueous systems is rather poor, since water may penetrate into the porous matrix and consequently decrease the oxygen permeability.

Hydrophobic sol–gels based on organically modified precursors avoid the penetration of water into the matrix. Such materials (also referred to as ormosils or ormocers) are an attractive alternative matrix for embedding indicators, especially for sensing gaseous species [17, 18]. The hydrophobicity of the materials may be adjusted either by selection of the nature of the organic group introduced into the glass or by the ratio of modified and non-modified precursor. Ormosils contain fewer free silanol groups and consequently will be less densified over time. As a result they possess an improved long-term and storage stability. Hydrophobic sol–gels prevent the penetration of charged species into the matrix and enhance the selectivity of gas sensors.

As described by Liu et al., ormosils that are soluble in methylene chloride are obtained if the condensation of the sol–gel is interupted after a defined period of time [19]. The prepolymer can be obtained as a viscous oil from the reaction mixture. After drying it can be re-dissolved in methylene chloride along with indicators such as Pt(II)–octaethylporphyrin.

We have improved this procedure to produce long-term stable and fast responding oxygen micro-optodes. The solubility and stability of the new ormosils is guaranteed by (a) proper selection of end-capping precursors to minimise the number of reactive silanol groups and (b) by thermal treatment of the polymers. Luminescent ruthenium(II) complexes and platinum porphyrins are readily soluble in these polymers. These new oxygen-sensitive materials form the basis of fiber optic oxygen microsensors with improved performance with respect to mechanical stability, response time, signal intensity and sensitivity to oxygen.

Experimental

Reagents and Chemicals

Ruthenium(III) chloride hydrate, 4,7-diphenyl-1,10-phenanthroline (dpp) and sodium trimethylsilylpropanesulfonate (TMS) were obtained from Aldrich. Platinum(II)-octaethylporphyrin (PtOEP) was from Porphyrin Products (Logan, Utah). Phenyltrimethoxysilane (PTMS) and trimethylmethoxysilane (TMMS) were from ABCR (Karlsruhe, Germany). Analytical grade ethanol and chloroform were from Merck (Darmstadt, Germany). All chemicals were used without further purification. The ruthenium(II)–(tris-4,7-diphenyl-1,10-phenanthroline) complex with TMS as the

Table 1. Properties of p_{O_2} sensing films obtained from different batches of ormosils (indicator content 5 mM Ru[dpp]$_3$)

Polymer	Molar ratio of PTMS/TMMS (R)	Consistency	τ_0 (μs)	τ_0/τ_{air}	Photo stability	Comments
S1	18	rigid glass	5.3	1.76	high	sensing film cracks easily, low temperature coefficient
S2	7.2	glass (less rigid)	5.7	1.50	moderate	excellent adhesion on glass and polymeric supports
S3	3.6	sticky	5.8	1.96	poor	excellent adhesion on glass and polymeric supports; high temperature coefficient
S4	1.8	highly viscous liquid	5.3	2.61	poor	no stable films

counter-ion (referred to as Ru[dpp]$_3$ in the following) was prepared as described previously [20]. Nitrogen, oxygen and air (all >99.9% pure) were obtained from Air Liquide (Germany).

Preparation of the Ormosils

Phenyltrimethoxysilane (25 ml) was dissolved in 25 ml of ethanol and 6 ml of 0.1 M hydrochloric acid was added. The mixture was refluxed at 65 °C for 2.5 h. Then various amounts of TMMS were added (Table 1) and the reaction was continued for another hour.

After cooling, 300 ml of water were added to the reaction mixture to stop the reaction and to precipitate the crude prepolymer. An emulsion was formed during this step and after storage for at least 12 h the prepolymer was separated as a viscous oil on the bottom. The water phase was removed and the oily residue was dried and cured at 200 °C for 5 h. Depending on the respective ratio of PTMS to TMMS (*R*) the consistency of the materials obtained varies considerably (Table 1). The glass material *S1* was powdered and dried again for 12 h at 280 °C under vacuum to finalise the curing process and to remove all traces of volatile components from the polymer. The materials obtained are clear, transparent and soluble in dichloromethane, chloroform or acetone.

Preparation of Sensing Films

A ''cocktail'' was prepared by dissolving 0.5 g of the ormosil and 3.5 mg of Ru[dpp]$_3$ in 2.5 ml of chloroform. For a detailed investigation of the new oxygen-sensitive materials thin films were prepared by spreading the cocktails onto a transparent polyester foil with a spreading device (Coesfeld GmbH, Germany). The thickness of the dried sensing films was estimated to be 10 μm. After complete evaporation of the solvent the films were ready for use. For sterilisation experiments the inner walls of small glass bottles were coated with a thin film of a sensing layer based on S1.

Manufacturing of Micro-Optodes

The micro-optodes were fabricated by a procedure described elsewhere [8]. Gradient index silica fibers (100/140 μm) equipped with standard fiber connectors were used. Fiber tips with diameters ranging from 10 μm up to 50 μm were prepared by tapering the silica fibers in a small flame of a microtorch. A capillary puller (Bachhofer) was used to fix the fiber and keep the tension constant during the melting process. The shape of the taper may be adjusted by either changing the temperature of the flame or the tension applied to the fiber. The oxygen-sensitive coating was deposited by dipping the fiber tip into the sensing cocktails described above. After evaporation of the solvent the fiber tips were inserted into an oven at a temperature of 190 °C for 10 min to remove all traces of volatile components. Micro-optodes were prepared with 5 mM Ru[dpp]$_3$ dissolved in *S1* (*M1*) and 5 mM PtOEP also dissolved in *S1* (*M2*). The coated fiber tips were fixed in a glass capillary for better handling during the measurements.

Instrumentation

The sensing films were characterized with a fiber optic set-up. A bifurcated glass fiber bundle with an active diameter of 2 mm [NA (numerical aperture) 0.46] was connected to a thermostatic flow-through cell where pieces of the sensing films (diameter 10 mm) were fixed. A bright blue LED (NSPB 500, λ_{max} 470 nm, Nichia, Nürnberg) equipped with a blue glass filter (BG 12, Schott) was selected as light source. A compact photomultiplier tube (H5702, Hamamatsu, Germany) equipped with a long pass cut-off filter (OG 570, Schott) was used to detect the luminescence signal. The average luminescence lifetime was measured in the frequency domain and a single modulation frequency was used. Sine wave modulation of the LED at a frequency of 45 kHz and phase detection were performed with a dual phase lock-in amplifier (DSP 830, Stanford Research Inc.).

Micro-optodes were characterised by using a commercially available lifetime-based fiber optic oxygen meter (MICROX 1, PreSens GmbH, Germany). The optoelectronic set-up of the instrument was described in detail elsewhere [21, 22] and is shown in Fig. 1. The same blue-green LED (NSPG 500, λ_{max} 505 nm, Nichia, Nürnberg) was used for excitation of both Ru[dpp]$_3$ and PtOEP based micro-optodes. The modulation frequencies were 37 kHz for sensor *M1* and 5 kHz for sensor *M2*.

Characterisation of the Sensors

Calibration curves for both sensing films and micro-optodes were determined in the gas phase with humidified gas mixtures. Defined partial pressures were adjusted by mixing air, oxygen and pure

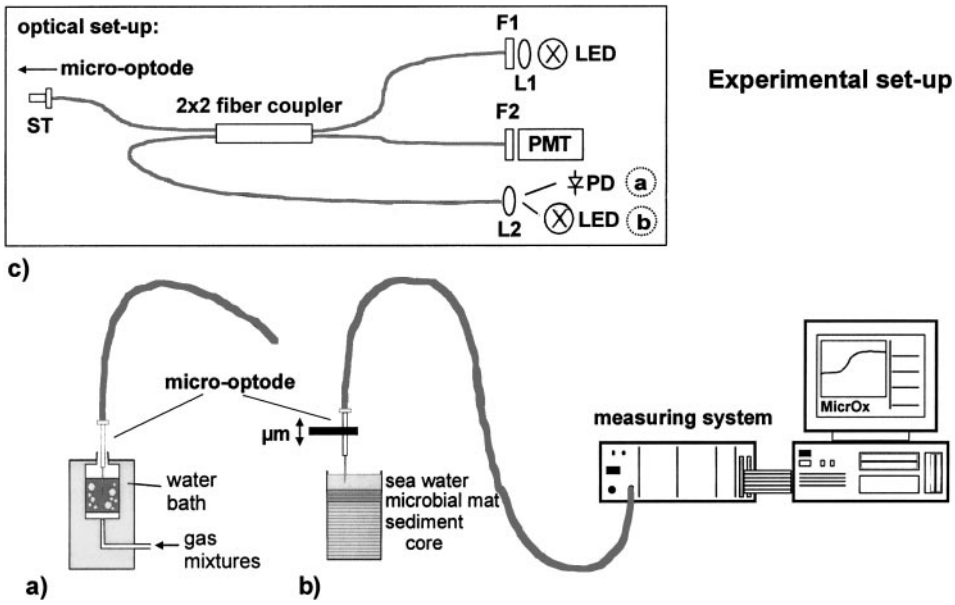

Fig. 1. Schematic drawing of the optical unit of the MICROX1 (LED, blue-green LED equipped with a lens (*L1*) and a blue short-pass filter (*F1*) for excitation; *PMT* photomultiplier module, *LED* (b) red-emitting LED for phase referencing; *PD* photodiode for referencing drifts of the LED; *ST* standard fiber connector); measuring set-up used for working with micro-optodes; (a) calibration chamber; (b) measuring of oxygen profiles in a sediment core (redrawn from [9])

nitrogen by means of mass flow controllers. The sensing films were fixed in a thermostatic flow-through cell. All measurements were performed at a temperature of 22 °C.

For investigation of photostability, the sensing films were illuminated under air with the focused light of a 150 W halogen lamp.

Results and Discussion

Selection of the Indicators

The $Ru[dpp]_3$ complex was selected as indicator because it has an extraordinarily high quantum yield, a long luminescence lifetime (appr. 6 µs in absence of oxygen) and is efficiently excitable with the blue or even the blue-green LED. Its lipophilic properties make it insoluble in water but readily soluble in many hydrophobic polymers. Trimethylsilylpropanesulfonate was selected as lipophilic counter-ion to enhance the solubility of $Ru[dpp]_3$ in the ormosils.

The second indicator chosen was PtOEP. Its outstanding long luminescence lifetime (approx. 90 µs in absence of oxygen) guarantees a high quenching efficiency and allows the development of oxygen micro-optodes for detection of traces of oxygen, with sufficiently high resolution.

Selection of the Polymer Precursor

From the many potentially useful precursors which have already been used for synthesis of ormosils we have selected phenyl-substituted PTMS as the most promising candidate for design of soluble sol–gels. We were not able to make soluble methyl-substituted ormosils with our procedure. After thermal treatment the methyl substituted polymers obtained were only swellable in apolar solvents. We think that the phenyl groups cause a large distance between the free silanol groups, which limit the level of cross-linking in the polymer network. Furthermore, that the presence of aromatic groups improves the photostability of the oxygen-sensing materials, is also known from sensing materials based on polystyrene. Phenyl substitution of the ormosil glasses will also improve the solubility of our indicators in the matrix and will therefore allow the fabrication of highly luminescent sensing materials.

TMMS was selected as the optimal end-capping agent. Hexamethyldisiloxane, which is formed as a by-product by dimerisation, can be removed from the crude polymer by simple evaporation, owing to its low boiling point (99 °C).

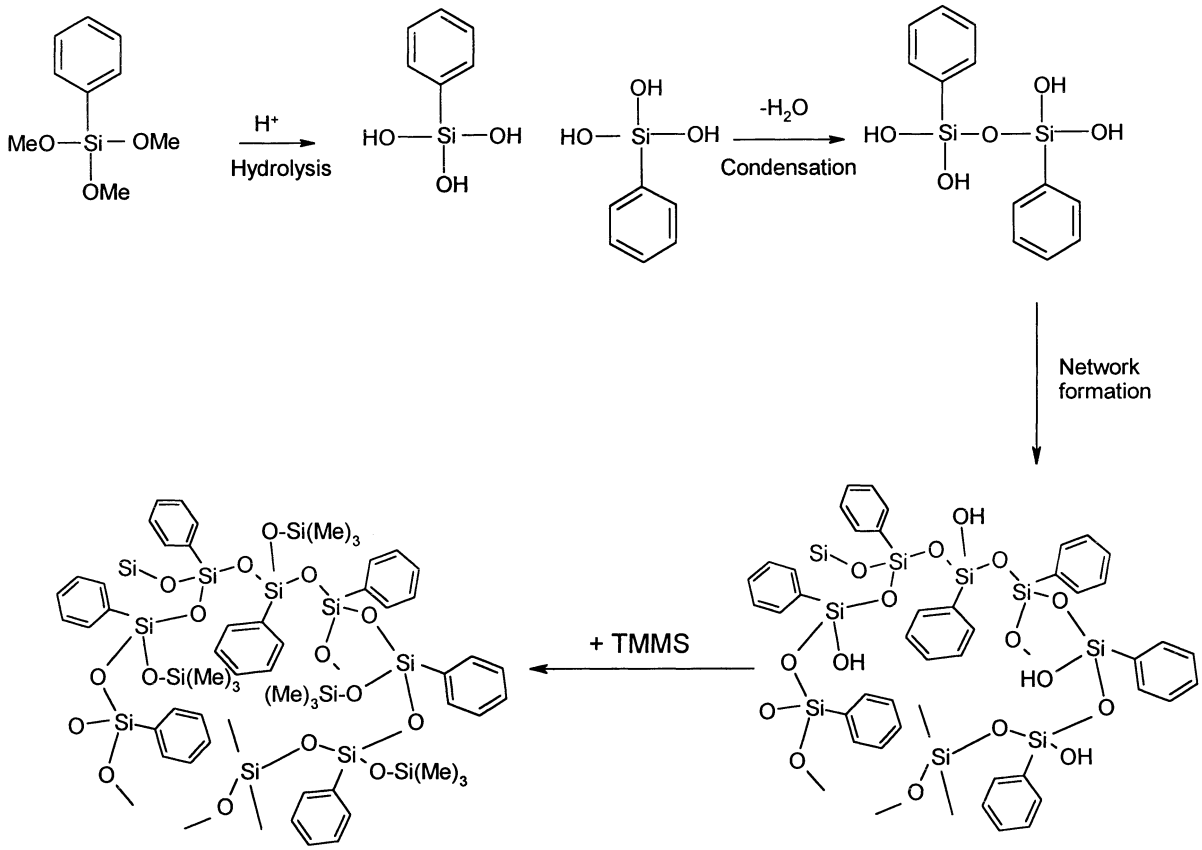

Fig. 2. Scheme of the sol–gel process and microstructure of the phenyl substituted soluble ormosils with end-capping trimethylsilyl groups

Synthesis of Ormosils

The synthesis of the new ormosils is simple and fast. The reaction steps are schematically shown in Fig. 2. The temperature during the hydrolysis and condensation must be kept constant to obtain polymers with identical properties: 65 °C has been found optimal for obtaining a sufficiently fast condensation and cross-linking. An excess of water was added to the reaction mixture after 3.5 h to stop the reaction. An emulsion was formed during this step and the crude polymer was separated as a highly viscous oil from the solvent after storage for at least 12 h at room temperature.

An important variation from the procedure described by Liu et al. [19] was the addition of TMMS to the reaction solution as an end-capping agent (Fig. 2). This step is the basis for obtaining readily soluble sol–gel glasses even if cross-linking is completed by a long thermal treatment of the crude prepolymers. A temperature of 200 °C was found optimal for finishing the cursing process. It was found that long-term exposure at temperatures higher than 300 °C damages phenyl-substituted ormosils. They become insoluble and yellow and show a strong intrinsic green fluorescence if excited with blue light. We assume that this is caused by oxidation of the phenyl groups, which are not stable under such harsh conditions. The thermal treatment is the most crucial step in the fabrication process for realising a sufficient batch to batch reproducibility.

Effects of TMMS Content

It was found that the molar ratio of the precursor PTMS and the end-capping agent TMMS (now denoted by R) tunes the mechanical and photophysical properties of the polymers (Table 1). Rigid glasses were obtained only with a low content of TMMS (*S1*). With decreasing *R* the materials lose their rigidity and become more flexible (*S2*). If a very large excess of TMMS is used, the material becomes sticky (*S3*) or even liquid (*S4*).

Sensing films prepared from *S1* material are rigid and crack easily. Nevertheless, stable films can be

realised if the thickness of the layer is less than 10 µm. Films obtained from *S2* and *S3* do not crack, and show excellent adhesion to the polyester support and also to tapered optical fibres.

Since *R* considerably affects the consistency of the ormosils, a correlation between *R* and the quenching efficiency was expected. The correlation between *R* and the oxygen sensitivity [expressed as $(\tau_0 - \tau_{air})/\tau_{air}$] was examined. Surprisingly, the lowest sensitivity was given by the flexible films prepared with moderate amounts of TMMS (*S2*). The sensing material based on polymer *S1* combines mechanical stability and a high oxygen sensitivity and was therefore selected as most suitable for micro-optodes.

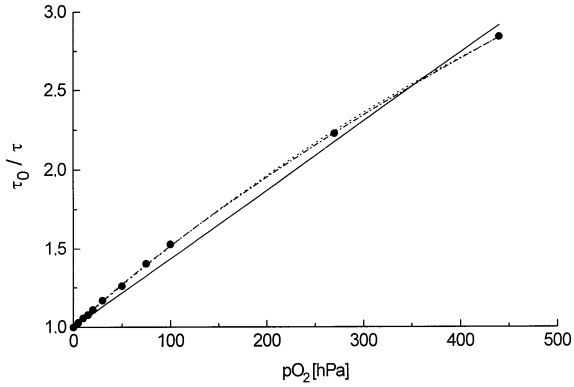

Fig. 3. Description of the Stern–Volmer calibration curve of an S1/Ru[dpp]$_3$ oxygen optode; solid line: Stern–Volmer model [Eq. (2)], dotted line: two-site model [Eq. (3)], dashed line: adapted two-site model [Eq. (4)]

Solubility

The use of soluble ormosils instead of curable precursor solutions makes fabrication of the optodes simple and improves the reproducibility of the sensors. A stock solution of the sensor ''cocktail'' (polymer indicator solution) can be stored over periods of at least a few months without altering its properties, and enables the reproducible manufacturing of different batches of sensors over a long period. It is also possible to prepare the polymer in large quantities, improving the batch to batch reproducibility from sensor to sensor. Sensing materials based on sol–gel glasses are commonly insoluble in all solvents due to their high degree of cross-linking. The new ormosils described here behave like linear organic polymers and are soluble in many polar solvents. This is mainly due to the fact that the addition of the end-capping agent minimises the level of cross-linking.

The new ormosils are not only soluble in methylene chloride as already described by Liu et al. [19], but also in chloroform, acetone, ethyl methyl ketone, toluene, ethyl acetate and cyclohexane. *S1* is also swellable in non-polar solvents such as diethyl ether, n-hexane and petrol ether. The polymers are completely insoluble in water, ethanol and methanol. For manufacture of oxygen-sensitive films and the micro-optodes the new ormosils were dissolved in chloroform since it is also an excellent solvent for the luminescent indicators used.

Description of Calibration Curves

The Stern–Volmer calibration curves of all the sensors show the typical non-linearity which is observed for many other oxygen optodes described in the literature [23]. Fig. 3 shows the lifetime-based Stern–Volmer plots of sensing films prepared from *S1*. The average lifetimes was calculated from a single frequency measurement by using Eq. (1):

$$\tau = \frac{\tan\Phi}{2\pi f_{mod}} \tag{1}$$

where f_{mod} is the respective modulation frequency.

We know that this relation only reflects the true luminescence lifetime if the indicator shows a single exponential decay. The calibration curve in Fig. 3 was evaluated with three different models which had already been successfully used in optical oxygen sensing. It is obvious that use of the Stern–Volmer equation [Eq. (2)] does not fit the calibration curve well ($\chi^2 = 0.099$).

$$\frac{\tau_0}{\tau} = 1 + k_{sv} p_{O_2} \tag{2}$$

The best correlation was obtained if the two-site model of Carraway et al. [23] [Eq. (3)] was used ($\chi^2 = 0.0027$).

$$\frac{\tau_0}{\tau} = \frac{f_1}{1 + k_{sv_1} p_{O_2}} + \frac{f_2}{1 + k_{sv_2} p_{O_2}} \tag{3}$$

This model is based on the assumption that the indicator is distributed in the polymer matrix at two different sites and each fraction (f_1, f_2) shows a different quenching constant (K_{sv1}, K_{sv2}). For practical use this model is not very convenient since it has too many parameters which have to be calibrated. Therefore we have also tried to use an adapted two-site

model which was successfully used for polystyrene-based sensors previously [Eq. (4)] [8].

$$\frac{\tau_o}{\tau} = \frac{f_1}{1 + k_{sv} p_{O_2}} + f_2 \qquad (4)$$

In this model one fraction of the luminophore is non-quenchable ($K_{sv2} = 0$). It was found that this model also describes the calibration curve with sufficient accuracy ($\chi^2 = 0.0077$). It was therefore selected for calibration of the micro-optodes. For a defined indicator/polymer combination the fractions f_1 and f_2 have constant values of 0.85 and 0.15 respectively (the shape of the calibration curves and therefore f_1 and f_2 are not affected by temperature changes) and need not be calibrated. Under these conditions a two-point calibration (typically performed with deaerated and air-saturated water) is sufficient to describe the calibration curves of the sensing films and the micro-optodes.

Photostability

Photostability of the sensing material is a crucial factor for a micro-optode to work well. Due to the efficient coupling of excitation light into the optical fiber and the focusing effect of the tapered fiber, extraordinary high illumination densities of up to 50 mW/cm^2 can be achieved at the sensing tip. Only exceptionally photostable materials can survive such conditions over a measuring period of several hours or even days without any change of the calibration curve.

Therefore the correlation between photostability and TMMS content in the reaction mixture was investigated. The luminescence lifetime in absence of oxygen was measured as the variable parameter during this experiment. The widespread assumption that photobleaching has no effect on lifetime measurements is frequently not true in practice, since photoproducts may quench the excited state of the oxygen indicator or show an intrinsic fluorescence.

We found that a high amount of TMMS reduces the photostability of the immobilised Ru[dpp]$_3$ in the sensing films significantly (Fig. 4). Sensing materials based on *S1* show the best photostability. We assume that the decrease in the ratio of phenyl to methyl substituents in the matrix is responsible for this behaviour. It was also found that with increasing indicator concentration the photostability is decreased. This agrees with the assumption that the photoproducts act as a quencher of the luminescence.

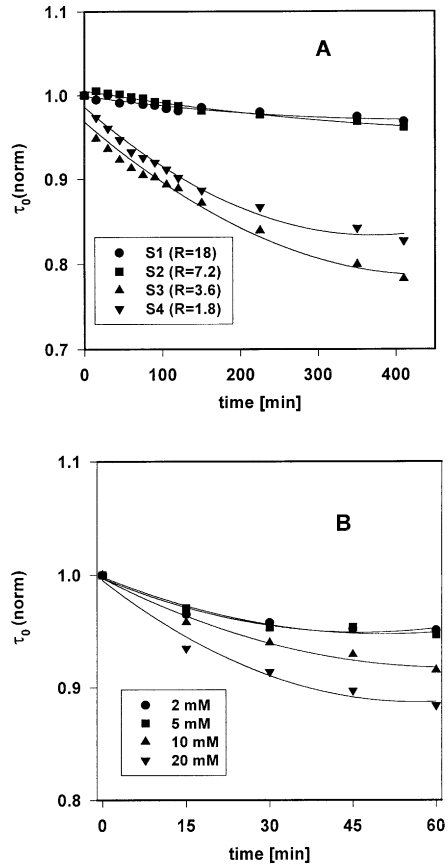

Fig. 4. Photostability of Ru[dpp]$_3$ dissolved in phenyl-substituted ormosils: correlation with PTMS/TMMS ratio R (A); correlation with indicator concentration (B)

Sterilisation of the Ormosils

As mentioned above, oxygen micro-optodes described previously can not be sterilised by autoclaving. Nevertheless, for application of the sensors in cell cultures and in medical research, sterilisation is essential to avoid contamination of the sample. It was found that sensing materials based on *S1* can be autoclaved several times without problems. Autoclaving experiments were performed with 10 small glass bottles where the inner wall was coated with the oxygen-sensitive material. The bottles were autoclaved 10 times (sterilisation conditions: 1 h at 130 °C and 1.5 atm). Under these conditions all microorganisms will be completely destroyed. The luminescence lifetime in the absence of oxygen (τ_0, reflecting the effect of thermal treatment of the indicator) and the quenching efficiency [$(\tau_0 - \tau_{air})/\tau_{air}$], reflecting the oxygen permeability of the matrix) were determined after each sterilisation cycle. The sensing films

remained mechanically stable, transparent and highly luminescent during sterilisation. Only a small drift in the oxygen sensitivity (−8% after 10 cycles) as well as of τ_0 (−3% after 10 cyles) was found. The shape of the calibration curve is unchanged during this procedure, allowing a two-point recalibration after each sterillisation cycle.

Storage Stability

The plain ormosils, as well as oxygen optodes based on *S1*, may be stored at room temperature for at least one year. The ormosils do not lose their solubility with time. Sequential manufacturing of oxygen-sensitive films from the same batch of *S1* over a period of 6 months resulted in sensing films with deviations of less than 2% in k_{sv} and τ_0. Similar deviations were obtained when *S1* based optodes were stored in a refrigerator for a period of 1 year. Optodes based on *S3* and *S4* age slightly over time, maybe because of continuous loss of oligomers with a low molecular weight.

Characterisation of the Micro-Optodes

On the basis of the results described above, *S1* was selected as the optimal matrix for design of oxygen micro-optodes. It was expected that such sensors will combine the advantages of microsensors based on $Ru[dpp]_3$ dissolved in polystyrene (high luminescence signal and very good photostability) and micro-optodes where PtOEP is dissolved in polystyrene (high oxygen sensitivity) [9]. A very fast response, the possibility of sterilisation and good mechanical stability should also be realised with the new sensing material.

Two micro-optodes were investigated *M1* is based on $Ru[dpp]_3$ dissolved in *S1* and allows oxygen measurement even in oversaturated oxygen systems, whereas *M2*, based on PtOEP dissolved in *S1*, was specially designed for the sensitive measurement of trace amounts of dissolved oxygen.

In contrast to the sub-µm sensors described by Kopelman et al. [24, 25] the optical fiber is not used only for excitation of the sensing layer but also guides the luminescence signal back to the photodetector. Therefore *in vivo* measurements in complex biological samples are possible with this type of sensor. Multi-mode gradient index silica fibers with a core diameter of 100 µm were selected as optimal, since they allow

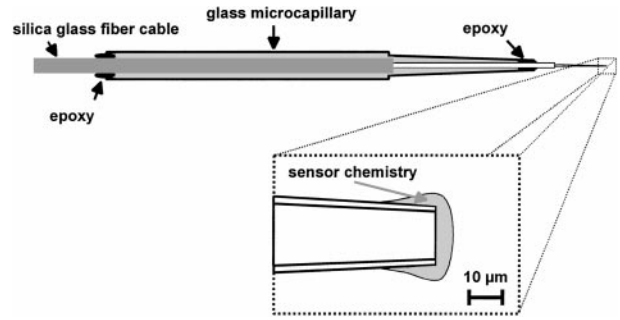

Fig. 5. Cross-section through a fiber optic oxygen microsensor tip (partially redrawn from [9])

efficient coupling of excitation light even when an LED is used as light source.

The tip diameter of a macro-optode typically ranges between 10 and 50 µm. This size is the optimal compromise to guarantee sufficiently high spatial resolution of the measurement, negligible disturbance of the sample, high luminescence signal and sufficient mechanical stability of the sensing tip. It is possible to prepare even smaller fiber tips but then the signal intensity becomes quite low, increasing the noise of the measurement. A cross-section through the tapered fiber tip is shown in Fig. 5. The thickness of the sensing layer deposited on the sensing tip was typically less than 2 µm. The sensing layer can be coated with a additional black gas-permeable layer which protects the sample from illumination and avoids the artificial stimulation of photosynthesis in phototrophic communities.

The new micro-optodes show a very fast response ($t_{90} = 250$ ms) (Fig. 6). A similar response behaviour in the gas phase and for dissolved oxygen in aqueous solutions has been observed. This is typical behaviour of microsensors with dimensions smaller than 50 µm and is in clear contrast to sensors with larger dimensions. The small dimensions of the fiber tip eliminate the diffusion limitation of oxygen transport through a boundary layer of water.

The adhesion between the silica fiber and the sensing layer is high, especially if very thin coatings are deposited. Coatings with a thickness of more than 2 µm show a tendency for cracking if the sensor penetrates rigid or cohesive samples. It can then be partially or completely removed from the fiber tip. If *S3* is used as the matrix instead on *S1* excellent adhesion of the coating onto the fiber tip is observed and cracking is no longer a problem. But micro-

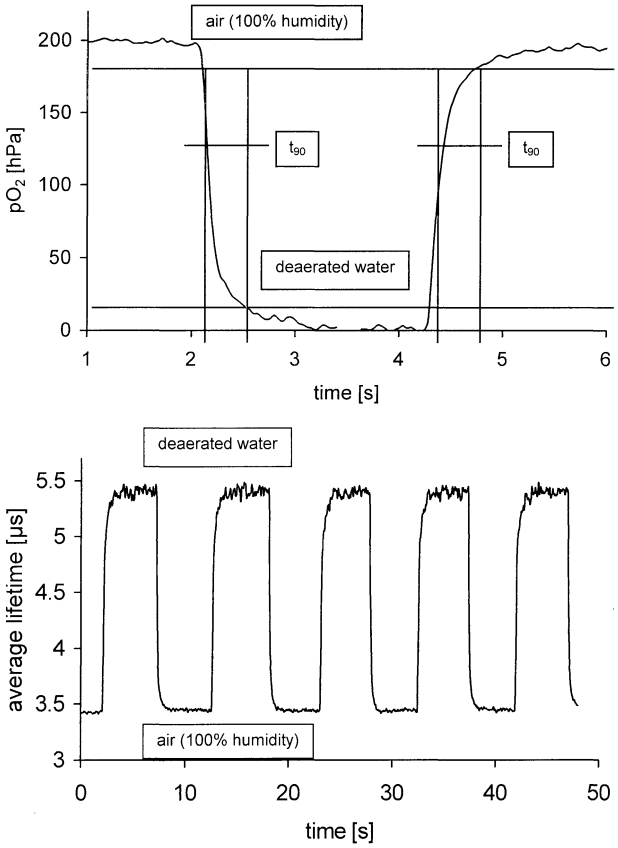

Fig. 6. Response behaviour of microsensor *M1* in the gas phase and in aqueous solution; the fiber tip was moved from humid air (lower line) into deaerated water (upper line), identical fast response times in water and the gas phase were found

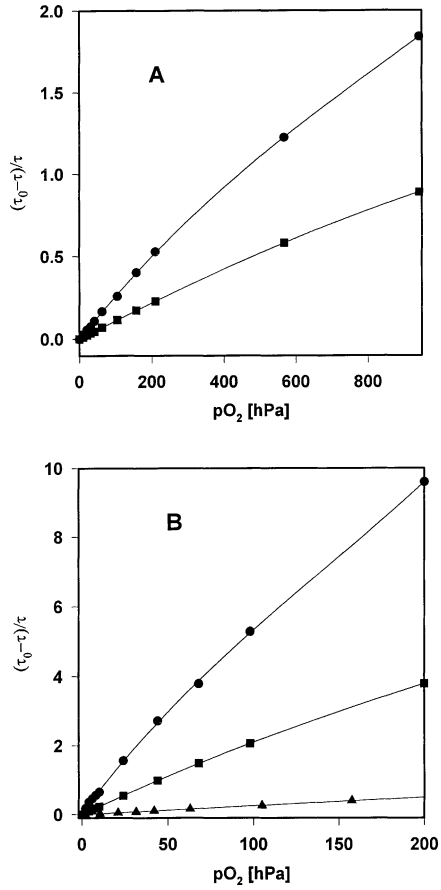

Fig. 7. Calibration curves of polystyrene- and ormosil-based optical oxygen microsensors; (A) (M11 squares, *M1* circles); (B) (M12 squares, *M2* circles, compared to *M1* triangles)

optodes based on *S3* show a poor photostability and consequently will not be described in detail.

The photostability of oxygen micro-optodes of the type *M1* is excellent (comparable to that of the polystyrene-based sensors or even better). Ten hours of continuous intense illumination with the light source of the fiber optic oxygen meter (a bright blue-green LED) results in a signal loss of approx. 2% in the intensity and less than 0.10° phase shift. This corresponds to a relative error in the determination in pO_2 of approx. 2 hPa. Sequential illumination will further enhance the long-term stability of the sensors.

From Fig. 7 it is obvious that sensor *M1* shows about three times higher sensitivity than polystyrene-based micro-optodes (Fig. 7a). The quenching efficiency may be further enhanced by a factor of two if the fiber tips are heated to 200 °C for at least 10 minutes. Unfortunately a certain fraction of the $Ru[dpp]_3$ does not survive under these harsh conditions, resulting in non-reproducible calibration curves of the sensors.

When PtOEP dissolved in *S1* is used as the sensing coating very sensitive oxygen micro-optodes (*M2*) were obtained (Fig. 7b). The detection limit of *M2* is 0.02 hPa, corresponding to 1 ppb of dissolved oxygen. The use of phosphorescent palladium porphyrins (with luminescence lifetimes up to 1 ms) instead of PtOEP would result in micro-optodes with even much lower detection limits. Sensor *M2* is the optimal choice to control anoxic conditions in living systems or to find anoxic sites in heterogeneous microbial communities. Such a high resolution measurement of trace levels of oxygen is impossible with micro-electrodes, owing to the small signals in the femtoampere range, and can only be performed with the new micro-optodes.

Table 2 compares the properties of oxygen micro-optodes described in the literature and our new

Table 2. Comparison of polystyrene- and ormosil-based oxygen micro-optodes

Sensor	M11 [8]	M1	M12 [9]	M2
Indicator/matrix	$Ru[dpp]_3$/polystyrene	$Ru[dpp]_3$/S1	PtOEP/polystyrene	PtOEP/S1
τ_0 (μs)	5.3	5.1	90	88
$(\tau_0-\tau_{air})/\tau_{air}$	0.23	0.53	3.8	9.6
Detection limit (hPa)	1.5	0.5	0.1	0.03
Photostability	high	very high	moderate	moderate
Signal intensity	high	high	moderate	moderate
Response time (t_{90}, s)	3	0.25	3	0.25
Sterilisation at 130 °C	not possible	possible	not possible	not tested

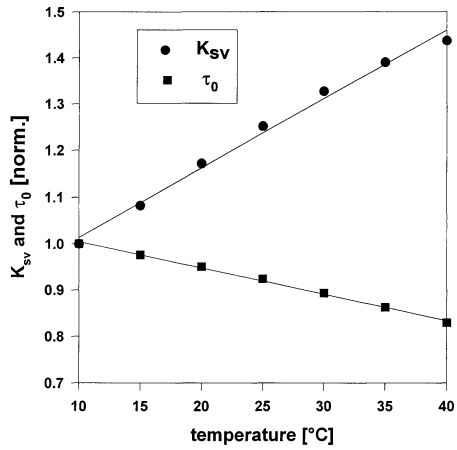

Fig. 8. Temperature behaviour of the parameters of the calibration function [Eq. (4)] for oxygen micro-optodes of type *M1*

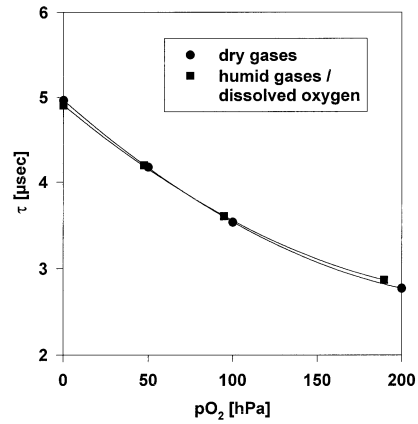

Fig. 9. Identical response curves of a microsensor of type *M1* in a dry and humid environment and in aqueous solution

sensors. It is evident that the new micro-optodes of type *M1* show optimal performance and cover almost the whole range of applications in medical and biological research.

The effect of temperature on the behaviour of the *M1* type micro-optodes was investigated in the range 10–40 °C, which covers the conditions for most biological and medical applications. Since the adapted Stern–Volmer equation [Eq. (4)] was found useful for calibration of the micro-optodes the temperature coefficients of τ_0 and K_{sv} were determined separately. It was found that temperature fluctuations have a more crucial effect on K_{sv} (+1.4% per degree) than on τ_0 (−0.6% per degree). The temperature has an almost linear effect on both parameters of the calibration function, as shown in Fig. 8.

The calibration function of the new micro-optodes is almost identical for measurement in the gas phase and for dissolved oxygen (Fig. 9). Humidity also has only a very small effect (< 2%) on the response of the sensors. The very hydrophobic nature of the polymer protects the sensor and minimises the uptake of water. Gas phase calibration is possible even for application in aqueous solutions.

Interferences were found only from sulfur dioxide (a notorious fluorescence quencher) and organic solvents which may swell the ormosil matrix.

The measurement of the phase shift as an oxygen-sensitive parameter instead of the luminescence intensity simplifies the handling of microsensors and reduces the number of potential errors. Fiber bending, microbending of the fiber tip and intensity fluctuations in the optoelectronic unit are completely referenced and have no effect on the signal. Furthermore, back-scattered light from the sample or intensity fluctuations caused by light absorption (a typical problem with dense phototrophic communities or blood) also do not shift the phase angle. Only significant levels of intrinsic sample fluorescence reduce the phase signal and result in higher apparent oxygen levels. From former investigations it is known that in dense phototrophic communities *chlorophyll a* can produce

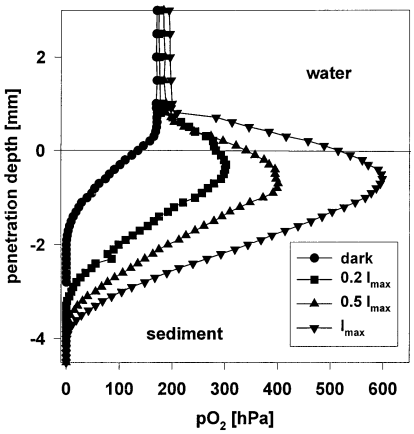

Fig. 10. Example of a high resolution measurement of oxygen gradients in a freshwater sediment core. The sample was taken from a depth of 1 m and was covered with a 2 mm layer of green algae. The oxygenation in the sediment was studied under different levels of illumination (from the dark up to I_{max}), simulating the varying natural conditions over a full day

a significant background fluorescence which may disturb the measurement. The use of an additional short-pass filter in front of the photomultiplier (cut-off wavelength 650 nm) overcomes this problem. It is also possible to coat the fiber tip with a black isolating layer. Nevertheless deposition of such an optical isolation complicates the fabrication process, increases the diameter of the fiber tip, makes the sensor slower and results in a lower signal intensity.

Another advantage of lifetime measurements compared to intensity measurements is the minimal influence of photobleaching. Deviations in the calculated oxygen level caused by photobleaching are lowered by a factor of five if the phase shift is used as the signal instead of the luminescence intensity.

Examples for the successful application of the new ormosil-based micro-optodes are high scale sensing of oxygen gradients in marine and freshwater sediments (Fig. 10) or the control the oxygenation of brain tissue and tumours.

Conclusion

New soluble phenyl-substituted ormosils were prepared and characterised and their application in optical oxygen sensing was evaluated. They make the manufacture of optical sensors based on sol–gel coatings more flexible. The modification with end-capping groups and the thermal treatment minimise the number of free reactive silanol groups in the matrix and avoid aging during storage.

Sensors with reproducible properties (τ_0, K_{sv} and the shape of the calibration curves) can be easily prepared from a single batch of the solid polymer or from a polymer/indicator solution kept over a period of at least half a year. The polymers described are not only useful matrices for oxygen sensors but also for optical sensors for pCO_2, sulfur dioxide and ammonia.

The ormosil with the lowest content of TMMS (*S1*) was found to be an excellent matrix for design of good performance micro-optodes. The embedding of the $Ru[dpp]_3$ complex in *S1* results in fast responding sensors with a moderate quenching efficiency. This microsensor can be used for oxygen measurement from very low oxygen levels (detection limit 0.5 hPa) up to partial pressures of more than 1000 hPa. On the other hand micro-optodes based on PtOEP dissolved in *S1* allow the measurement of traces of dissolved oxygen and may be used to control anaerobic processes.

Compared to previously described oxygen micro-optodes, those based on ormosils combine outstanding features such as high sensitivity, very fast response, excellent photostability and sufficient mechanical stability and, are sterilisable. They can be produced more cheaply than micro-electrodes with comparable properties. The low price of such sensors allows a more widespread application of the microsensor technology, which is frequently limited by the high costs caused by the fragility of such small sensors. The new sensors are suitable for most applications in medical and biological research. Oxygen gradients with a spatial resolution of up to 20 µm can be measured. In combination with the fiber optic oxygen meter (MICROX1) the sensors can be used under laboratory conditions as well as in the field.

Examples for the use of new micro-optodes are the measurement of oxygen gradients in marine and freshwater sediments and microbial mats, the measurements of tumour oxygenation and the determination of oxygen contents in the eyes of rabbits.

Acknowledgements. We thank Gisela Hirlmeyer for technical support and Gerhard Holst and Oliver Kohls from Max Planck Institute of Marine Microbiology for discussion. Acknowledgement is also made to the European Commission for support within the project MICROMARE no. MASCT950029.

References

[1] B. B. Jørgensen, N. P. Revsbech, in: *Advances in Microbial Ecology*, Vol. 9, (K. C. Marshall ed.) Plenum Press, New York, 1986, p. 293.

[2] M. Kühl, B. B. Jorgensen, *Appl. Environ. Microbiol*. **1992**, *58*, 1164.
[3] N. P. Revsbech, B. B. Jørgensen, T. H. Blackburn, Y. Cohen, *Limnol. Oceanogr.* **1983**, *28*, 1062.
[4] D. DeBeer, J. P. R. A. Sweerts, *Anal. Chim. Acta* **1989**, *219*, 351.
[5] N. P. Revsbech, L. P. Nielsen, P. B. Christensen, J. Sorensen, *Appl. Environ. Microbiol.* **1988**, *54*, 2245.
[6] W. J. Whalen, J. Riley, P. Nair, *J. Appl. Physiol.* **1967**, *23*, 789.
[7] N. P. Revsbech, *Limnol. Oceanogr.* **1989**, *34*, 474.
[8] I. Klimant, V. Meyer, M. Kühl, *Limnol. Oceanogr.* **1995**, *40*, 1159.
[9] I. Klimant, M. Kühl, R. N. Glud, G. Holst, *Sens. Actuators* **B 1997**, *38–39*, 29.
[10] J. R. Bacon, J. N. Demas, *Anal. Chem.* **1987**, *59*, 2780
[11] G. A. Khalil, M. P. Gouterman, E. Green, *US Pat. 4,810,655*, 1989.
[12] D. B. Papkovsky, *Sens. Actuators* **B 1995,** *29*, 213.
[13] O. S. Wolfbeis, R. Reisfeld, I. Oeheme, *Structure and Bonding*'85. Springer Berlin Heidelberg New York Tokyo, **1996**, p. 51.
[14] C. J. Brinker, G. W. Scherrer, *Sol–Gel Science*, Academic Press, New York, 1990.
[15] G. O. Keeffe, B. D. MacCraith, A. K. McEvoy, C. M. McDonogh, J. F. McGilp, *Sens. Actuators* **B 1995**, **29**, 226.
[16] S. K. Lee, I. Okura, *Analyst* **1997**, *122*, 81.
[17] A. K. McEvoy, C. M. McDonagh, B. D. MacCraith, *Analyst* **1996**, *121*, 785.
[18] M. K. Krihak, M. R. Shariari, *Electr. Lett.* **1996**, *32*, 240.
[19] H. Y. Liu, S. C. Switalski, B. K. Coltrain, P. B. Merkel, *Appl. Spectrosc.* **1992**, *46*, 1266.
[20] I. Klimant, O. S. Wolfbeis, *Anal. Chem.* **1995**, *67*, 3160.
[21] G. Holst, M. Kühl, I. Klimant, *Proc. SPIE* **1995**, *2508*, *387.*
[22] G. Holst, M. Kühl, I. Klimant, *Sens. Actuators* **B 1997**, *38–39*, 122.
[23] E. R. Carraway, J. N. Demas, B. A. DeGraff, J. R. Baron, *Anal. Chem.* **1991**, *63*, 337.
[24] W. T. Tan, Z. Shi, R. Kopelman, *Anal. Chem.* **1994**, *64*, 2985.
[25] Z. Rosenzweig, R. Kopelman, *Anal. Chem.* **1996**, *67*, 2650.

Received June 12, 1998. Revision December 10, 1998.